Spin-dependent transmission of holes through periodically modulated diluted magnetic semiconductor waveguides

X. F. Wang and P. Vasilopoulos

Concordia University, Department of Physics,

Montréal, H3G 1M8, Canada

We study spin transport of holes through stubless or stubbed waveguides modulated periodically by diluted magnetic semiconductor (DMS) sections of width b_1. Injected holes of *up (down)* spin feel a *periodically modulated barrier (well) potential* in the DMS sections and have different transmission (T) coefficients. T oscillates with b_1 for spin-down and decreases fast for spin-up holes while the relative polarization P_r depends nearly periodically on the stub height. Using asymmetric stubs leads to a nearly *square-wave* pattern in T and to wide plateaus in P_r. T oscillates with the length between the DMS sections. With two DMS sections per unit, T shows periodically wide gaps for spin-down holes when a DMS width is varied. The results can be used to create efficient spin filters.

In recent years spin transport has attracted considerable attention as it offers a possibility for a new type of transistor [1], quantum computation and quantum logic [2]. A significant part of the work has concentrated on spin-polarized electronic transport through diluted magnetic semiconductors (DMS) [2] despite the fact that the reported experimental spin polarizations are very low, about 1%, and make the results controversial and attributable to extraneous effects. Experimental work [3] showed that DMS materials $Ga_{1-x}Mn_xAs$ can be in the metallic ferromagnetic phase with heavy holes as carriers for $0.03 \leq x \leq 0.05$.

In previous work [4] we demonstrated that the electronic transmission through periodically stubbed waveguides, in the presence of spin-orbit interaction, shows a rich structure and a spin-transistor behavior as a function of the stub parameters. Here we demonstrate similar effects in the transmission of heavy holes through waveguides made of many identical units each of which consists of a nonmagnetic part, A, followed by a DMS one, B, as shown in Fig. 1 (a). Stubs can be attached to either part but it is advantageous to attach them to part B.

The spin-structure for holes is obtained [5] self-consistently in reciprocal space. The hole interaction with magnetic impurities is described by the potential

$$U_{mag}(\mathbf{r}) = -I\sum_{\mathbf{i=1}}^{\mathbf{N_i}} \mathbf{s}(\mathbf{r}).\mathbf{S}(\mathbf{R_i})\delta(\mathbf{r}-\mathbf{R_i}), \tag{1}$$

where I is the $p-d$ exchange coupling constant, $\mathbf{R_i}$ denotes the positions of the N_i impurities Mn , uniformly distributed in the DMS layers, $\mathbf{S}(\mathbf{R_i})$ is the spin of the impurity, and $\mathbf{s}$ the spin of the hole. We assume the magnetization of each layer to be oriented along a single direction, each layer being in its ferromagnetic phase. Thus, the spin of the hole is well defined in this direction, being parallel (down) or antiparallel (up) to it. Integrating $U_{mag}(\mathbf{r})$ over z and x gives the effective potential $V_{mag}(y)$ in terms of the average magnetization $< \mathbf{M} >_\mathbf{j}$:

$$V^{\sigma}_{mag}(y) = V_0\sigma \sum_j < M >_j g_j(y), \tag{2}$$

where $g_j(y) = 1$ if y lies inside the j-layer, and $g_j(y) = 0$ otherwise; $\sigma = \pm 1$ for spin-up and spin-down holes, respectively, and V_0 is a sample-dependent parameter for the strength

of the potential. The total potential felt by a hole is $U^{\sigma}_{eff}(y) = [U_c(y) + V^{\sigma}_{mag}(y) + U_h(y)]$, where $U_c(y)$ is the confining potential, and $U_h(y)$ the Hatree hole-hole interaction potential. Setting $E_k = h^2k^2/2m^*$ the hole Hamiltonian in the DMS section becomes

$$H = E_k + U^{\sigma}_{eff}(y) \equiv \begin{bmatrix} E_k + U^{+}_{eff}(y) & 0 \\ 0 & E_k + U^{-}_{eff}(y) \end{bmatrix}$$

The direction of the spin polarization depends on that of $< \mathbf{M} >_{\mathbf{j}}$. We assume the latter is along the waveguide (y axis) or along the stub (x axis). Generally, $U^{\sigma}_{eff}(y)$ is not constant inside the DMS layer and depends on parameters such as the Mn density, the layer size, the temperature, etc. For simplicity we assume that $U^{\sigma}_{eff}(y)$ is constant and $U^{\pm}_{eff} = \pm V$. A y-dependent potential can be treated by considering a DMS layer as a seriers of equal-width 'flat' potential layers of unequal height. Even for high hole densities, the resulting wave functions can be well approximated [5] by those of a square well.

The subject of this paper is a transistor-like modulation of a spin current. Motivated by previous results on electronic stub tuners [4,6] we consider ballistic spin transport of holes through waveguides with double stubs attached to them as in Fig. 1 (a) or without stubs.

Since the Hamiltonian is diagonal in the spin index, we can consider the propagation of spin-up and spin-down holes inside the structure independently and denote the wave functions by ϕ^{+} and ϕ^{-}, repectively. In each region of Fig. 1 (c) we have $\phi^{\sigma}_n(x) = \sqrt{2/w}\sin(n\pi(x + w/2)/w)$, where w is the width of the region along x. Including spin we can write the eigenfunction ϕ^{σ}_1 of energy E in region I as

$$\phi^{\sigma}_1 = \sum_m \{a^{+}_{1m} e^{i\beta^{\sigma}_m y} + b^{+}_{1m} e^{-i\beta^{\sigma}_m y}\} \sin[c_m(x + c/2)] \tag{3}$$

Here $c_m = m\pi/c$ and $\beta^{\sigma}_m = [2m^*(E - U^{\sigma}_{eff}) - c^2_m]^{1/2}$. In region III ϕ_2 is given by Eq. (3) with the changes $1m \to 2m$, $U^{\sigma}_I \to U^{\sigma}_{III}$, and $y \to y - b_1$. In the stub region II, Eq. (3) remains valid with the changes $c \to h$, $U^{\sigma}_I \to U^{\sigma}_{II}$, and $x + c/2 \to x + h/2 - d$.

Matching the wave function and its derivative at $y = 0$ and $y = b_1$ connects the incident waves (to the left of region I) with the outgoing ones (to the right of region III) with a spin-dependent transfer matrix $\hat{M}$

$$\begin{pmatrix} a_{in}^{\sigma} \\ b_{in}^{\sigma} \end{pmatrix} = \hat{M}^{\sigma} \begin{pmatrix} a_{out}^{\sigma} \\ b_{out}^{\sigma} \end{pmatrix}. \tag{4}$$

In DMS layers the hole momentum β^{σ} is strongly spin-dependent; this results in a phase difference between the spin-up and spin-down wave functions and in the spin-dependence of the transfer matrix $\hat{M}^{\sigma}$. If we inject *unpolarized* holes to the left of the structure, we can obtain spin *polarized* outgoing holes to its right because the transfer matrix $\hat{M}^{\sigma}$ and the transmission T^{σ} depend strongly on the spin σ of the holes. Here are the results.

In Fig. 2 we plot T vs the stub width b_1 for the parameters given in the caption. As shown, for a simple unit the spin-up transmission T^{+} decreases very fast whereas the spin-down one T^{-} oscillates. This fast decrease can be used to filter out the spin-up holes. This result agrees qualitatively with that for an unconfined single DMS layer in the presence of a normal magnetic field [7]. For a composite unit ($b_1 \neq b_2$) the result is similar. An interesting feature is shown in the inset. $T^{\pm}$ oscillates with the length between the DMS segments, i.e., it shows *longitudinal* resonances as that of spinless electrons [8].

The values of l at which T^{+} maxima occur, l_m, in Fig. 2 can be utilized to maximize the gaps in the transmission. In Fig. 3 we show T vs b_1 for a waveguide with 40 composite units and two different temperatures. Any l_m value leads to a maximum gap as dephasing of the wave between the DMS and GaAs sections is maximal.

So far we considered waveguides without stubs. If we attach stubs, we obtain several interesting results. The first of them is shown in Fig. 4 where we plot, for *symmetric* stubs, the relative output polarization $P_r = (J_u - J_d)/(J_u + J_d)$ vs the stub height h, with J_u (J_d) being the up (down) current. As N increases the gaps become wider and deeper and reach a limit for $N = 6$. Notice how P switches, nearly periodically, between +1 and -1, as h is changed. This behavior can be understood by inspection of the inset where we plot separately the currents J_u and J_d vs h. Due to the large effective Zeeman splitting the dependence of $T^{+} \propto J_u$ and $T^{-} \propto J_d$ on h is different and translates directly to that of P_r.

Another interesting result is shown in Fig. 5 for *asymmetric* stubs where P_r is plotted

vs the asymmetry parameter d, cf. Fig. 1 (c). Notice the wide ranges of d in which P_r takes the values -1, +1, and 0. The nearly *square-wave* pattern of T shown in the inset is similar to that for electrons with spin neglected [6] or considered in the presence of spin-orbit interaction [4].

A qualitative understanding of the results shown in Figs. 2-5 is easily reached if we combine the basic idea of a stub tuner [9] and its refinements [6] with the effective, spatially modulated potential of Fig. 1 (b) which makes *holes of up (down) spin "see" a barrier (well)* when propagating through the DMS sections. In a stub tuner waves reflected from the walls of the stub, where the wave function vanishes, may interfere constructively or destructively with those in the main waveguide and result, respectively, in an increase or decrease of the transmission. Refining this idea showed [6] that using *asymmetric* double stubs the transmission of *spinless* electrons could be blocked completely. Combining several stubs leads to a nearly *square-wave* transmission as a function of the asymmetry parameter d. The same idea applies to the holes we consider here and the transmission shown in the inset of Fig. 5 is simply the result of this behavior. In addition, the large effective Zeeman splitting between the spin-up and spin-down holes readily explains the oscillations of T^- in Figs. 2-3, since spin-down holes "see" a well whereas spin-up holes "see" a barrier which results in $T^+ \to 0$ upon increasing its width. The behavior of P_r in Figs. 4-5 stems directly from that of J_u and J_d which have a different dependence on h or d due to the large Zeeman splitting. As for the *longitudinal* resonances of $T^\pm$ in Fig. 2 , they have the same origin as those for spinless electrons [8]: in essence they result from matching of the phase of the wave between the GaAs and DMS sections. In contrast, absence of this matching leads to the large gaps of T^- in Fig. 3. Finally, with regard to the temperature dependence of some of the results, the reduction (and rounding off) of the transmission peaks and of the gaps in Fig. 3 is expected and in line with that for electrons [4,6]; it can be offset by increasing the ratio of the Fermi to the thermal energy. An important question concerns the influence of the stub shape on the transmission output. But as in electronic stub tuners [4,6], we have verified that here too changing the stub shape does not change the transmission qualitatively; it

only alters its period when plotted, e.g., vs h, and several units are combined.

The results presented so far are valid when only a single mode propagates in the main waveguide. If more modes propagate, the transmission pattern becomes more complex but it is still possible to have a periodic output, as in Fig. 2, if b_1 is short enough that only a single mode penetrates in the stub [6]. Details will be given elsewhere.

The DMS devices, on which the observability of the results relies, could be fabricated using the recently developed low-temperature MBE technique [3] to grow a superlattice which could be etched perpendicularly to produce a surface superlattice. Then patterned gates can be deposited on its surface to control the shape of the stubs.

In summary, we combined the spin-dependent transmission through a DMS section with the basic physics of a stub tuner and applied it to hole transport through a stubless or stubbed waveguide. We showed that the large effective Zeeman splitting results in a spin-dependent transmission. The transmission of the spin-up holes can be blocked whereas that of the spin-down ones oscillates with the DMS width showing wide gaps. More important, in stubbed waveguides the relative polarization varies nearly periodically with the stub height, switching from -1 to +1, while the transmission shows a nearly *square-wave* pattern upon using *asymmetric* stubs. The results should lead to the creation of efficient spin filters.

We thank Dr. I.C. da Cunha Lima for helpful discussions. Our work was supported by the Canadian NSERC Grant No. OGP0121756.

REFERENCES

[1] S. Datta and B. Das, Appl. Phys. Lett. **56**, 665, (1990).

[2] J. M. Kikkawa and D. D. Awschalom, Phys. Rev. Lett. **80**, 4313 (1998); Y. Ohno, D. K. Young, B. Beschoten, F. Matsukura, H. Ohno, and D. D. Awschalom, Nature **402**, 790 (1999); R. Fiederling, M. Keim. G. Reuscher, W. Ossau, G. Schmidt, A Waag, and L. W. Molenkamp, Nature (London) *ibid* **402**, 787 (1999).

[3] F. Matsukura, H. Ohno, A Shen, and Y. Sugawara, Phys. Rev. B **57**, R2037 (1998).

[4] X. F. Wang, P. Vasilopoulos, and F. M. Peeters, Appl. Phys. Lett. **80**, 1400 (2002); Phys. Rev. B **65**, 165217 (2002).

[5] A. Ghazali, I. C. da Cunha Lima, and M. A. Boselli, Phys. Rev. B **63**, 153305 (2001).

[6] R. Akis, P. Vasilopoulos, and P. Debray, Phys. Rev. B **52**, 2805 (1995).

[7] K. Chang and F. M. Peeters, Solid State Commun. **120**, 181 (2001).

[8] G. Kirczenow, Phys. Rev. B **39**, 10452 (1988).

[9] S. Datta, Superlatt. Microstruct. **6**, 83 (1989).

FIGURES

FIG. 1. (a) A periodically stubbed waveguide (A=GaAs, B=DMS). (b) The effective potential V along the growth axis for spin-up (solid curve) and spin-down (dotted curve) holes. (c) A waveguide portion with two stubs (shaded areas). For a simple unit we have $b_1 = b_2$, for a composite one $b_1 \neq b_2$. The midpoints of h and c determine the asymmetry parameter d.

FIG. 2. Transmission T as a function of the stub width b_1 for a simple unit (solid and dotted curves) and for a composite one (dashed and dash-dotted curves, $b_2 = 50$ Åwith $l = 207.5$ Å.) The fast decreasing curves are for spins up (T^+), the oscillating ones for spins down (T^-). The inset shows T^+ (solid curve) and T^- (dotted curve) vs l (in units of 100 Å) of a stubless ($h = a = 250$ Å) waveguide with $b_1 = b_2 = 50$ Å, $V = 3$ meV, and $E_F = 4.48$ meV.

FIG. 3. Transmission T vs the width b_1 in a *stubless* ($h = a = 150$ Å) waveguide of 40 composite units ($b_2 = 30$ Å, $l = 142$ Å, $V = 16.5$ meV, $E_F = 12.5$ meV). The solid (dashed) curves show $T^{\mp}$ at the indicated temperatures.

FIG. 4. The relative output polarization P_r vs the stub height h for $V = 0.3$ meV, $E_F = 4.48$ meV, and temperature $T = 0.1$ K. N is the number of simple units ($b_1 = b_2 = 50$ Å). The inset shows $T^+ \propto J_u$ (solid curve) and $T^- \propto J_d$ (dotted curve) vs h.

FIG. 5. The relative output polarization P_r vs the asymmetry parameter d for a stubbed waveguide of 5 simple units ($b_1 = b_2 = 150$ Å, $l = 207.5$ Å, $h = 1014$ Å) at temperature $T = 0.1$ K with $V = 0.3$ meV and $E_F = 4.48$ meV. The inset shows T versus d with $b_1 = b_2 = 50$ Å and $l = 207.5$ Å. The solid (dashed) curves are for spin-down (spin-up) holes.

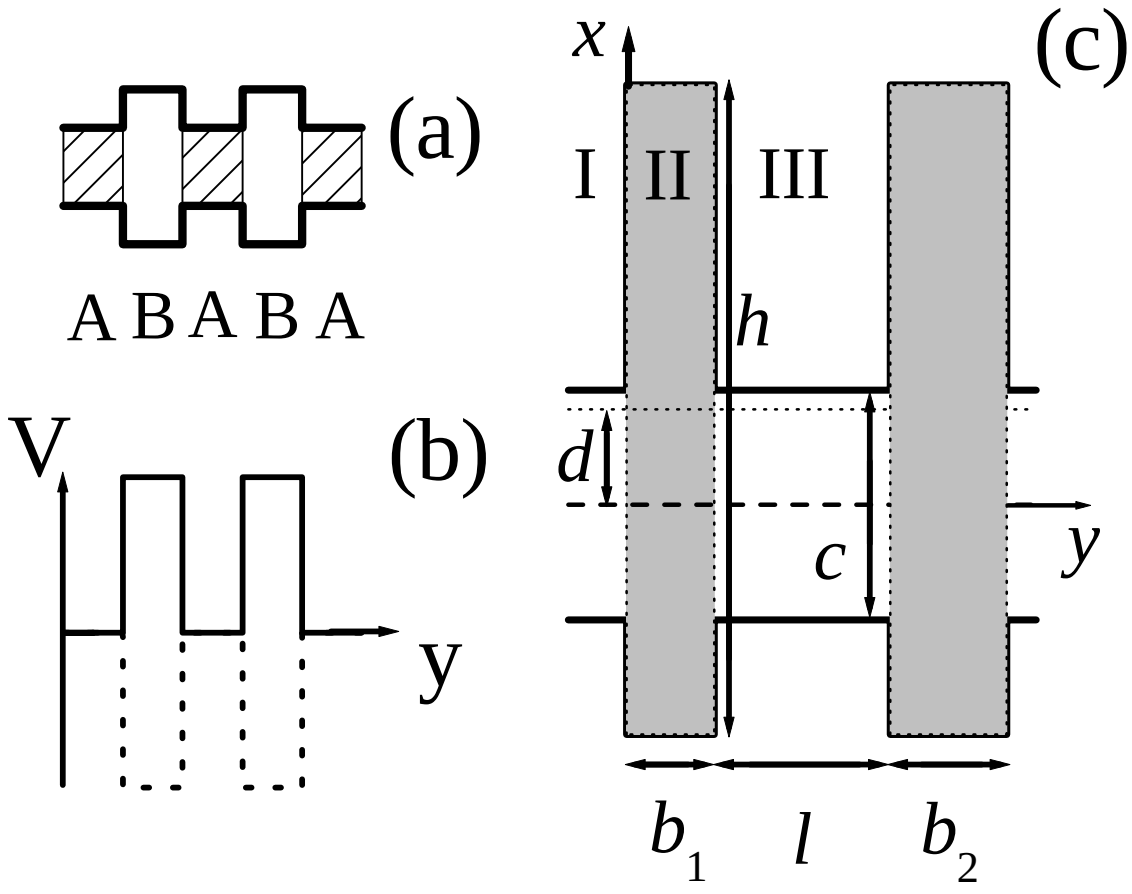
(a)
A B A B A
V
(b)
y
x
(c)
I
II
III
h
d
c
y
b_1
l
b_2

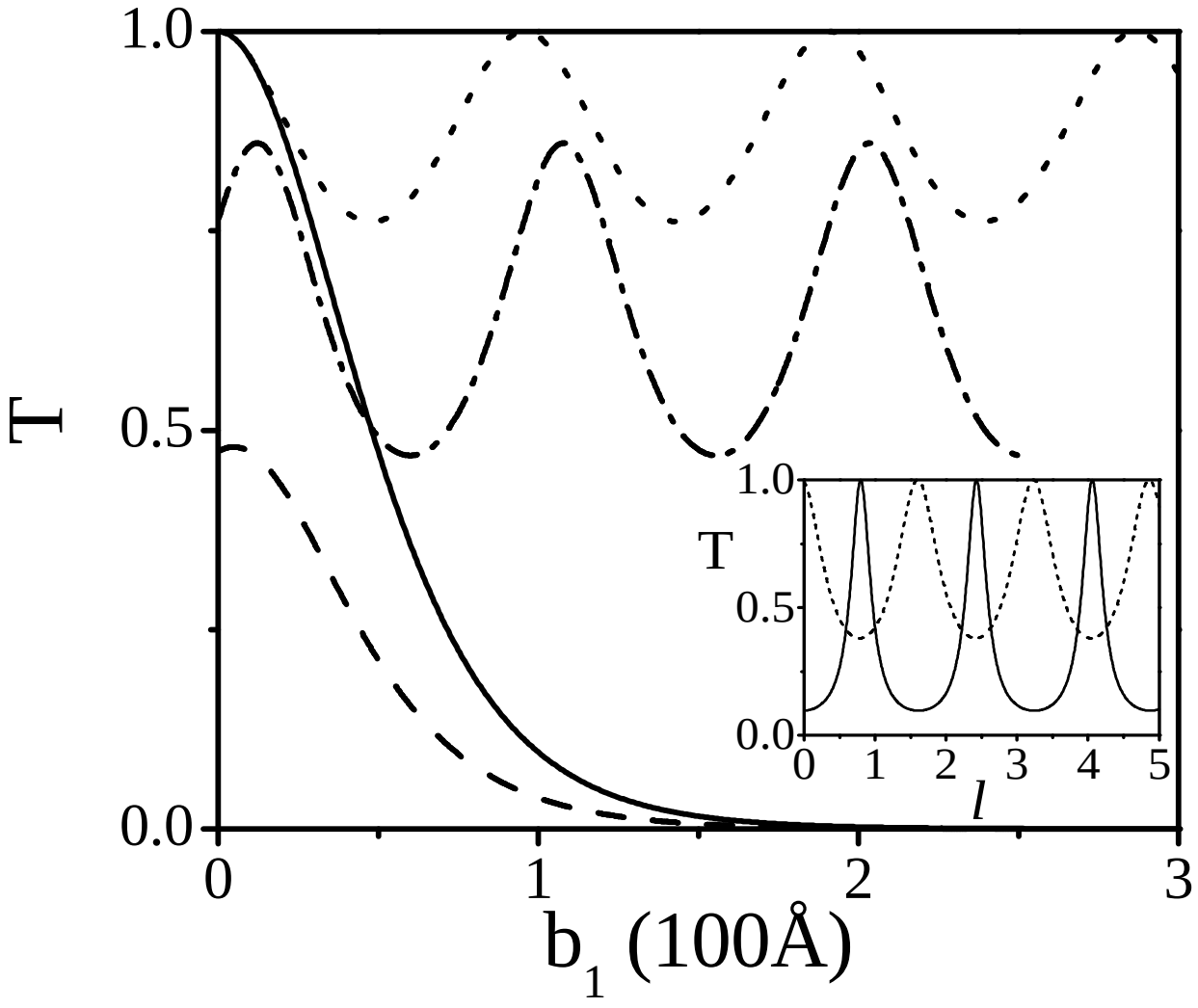

Fig.2, Wang and Vasilopoulos

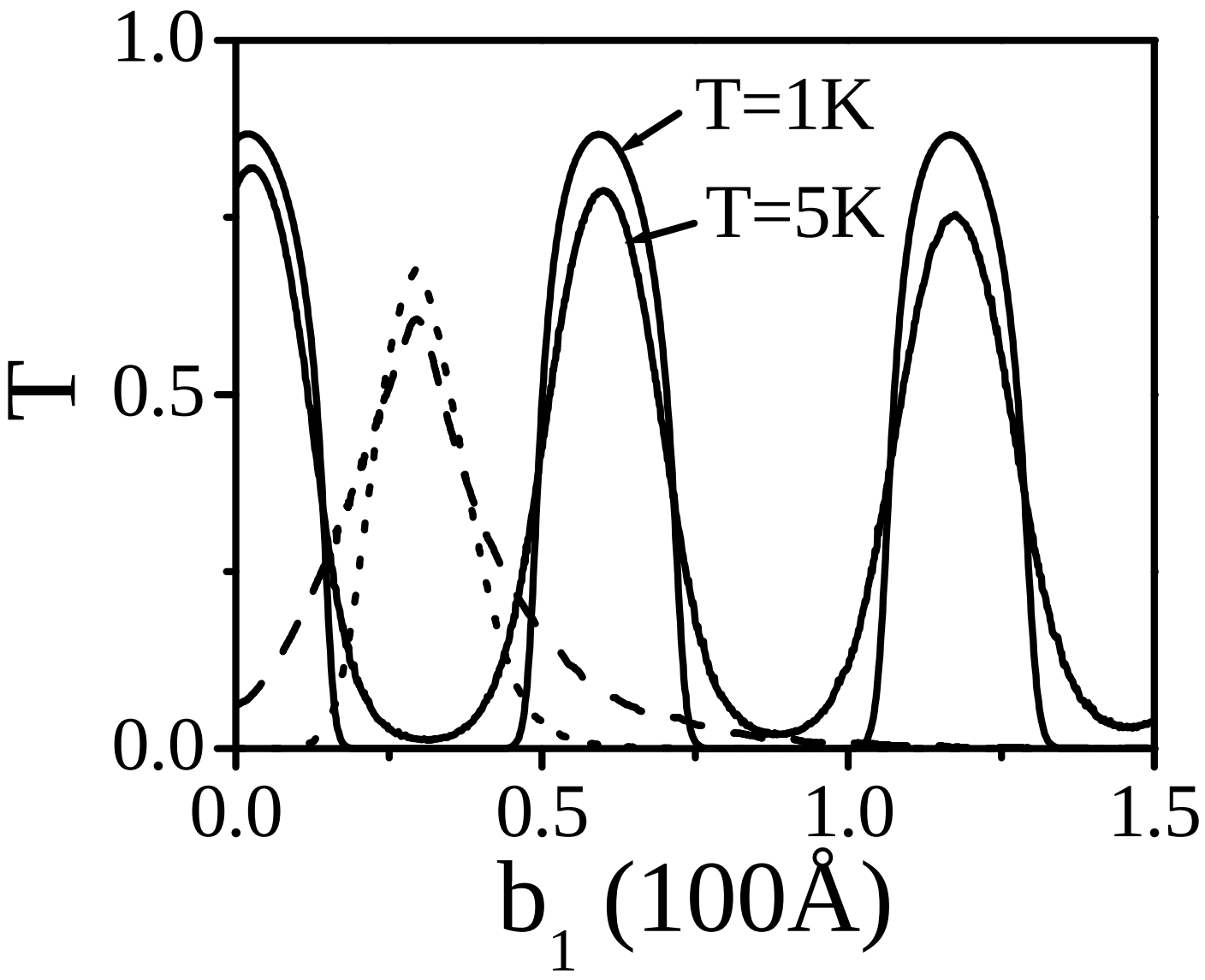

Fig.3, Wang and Vasilopoulos

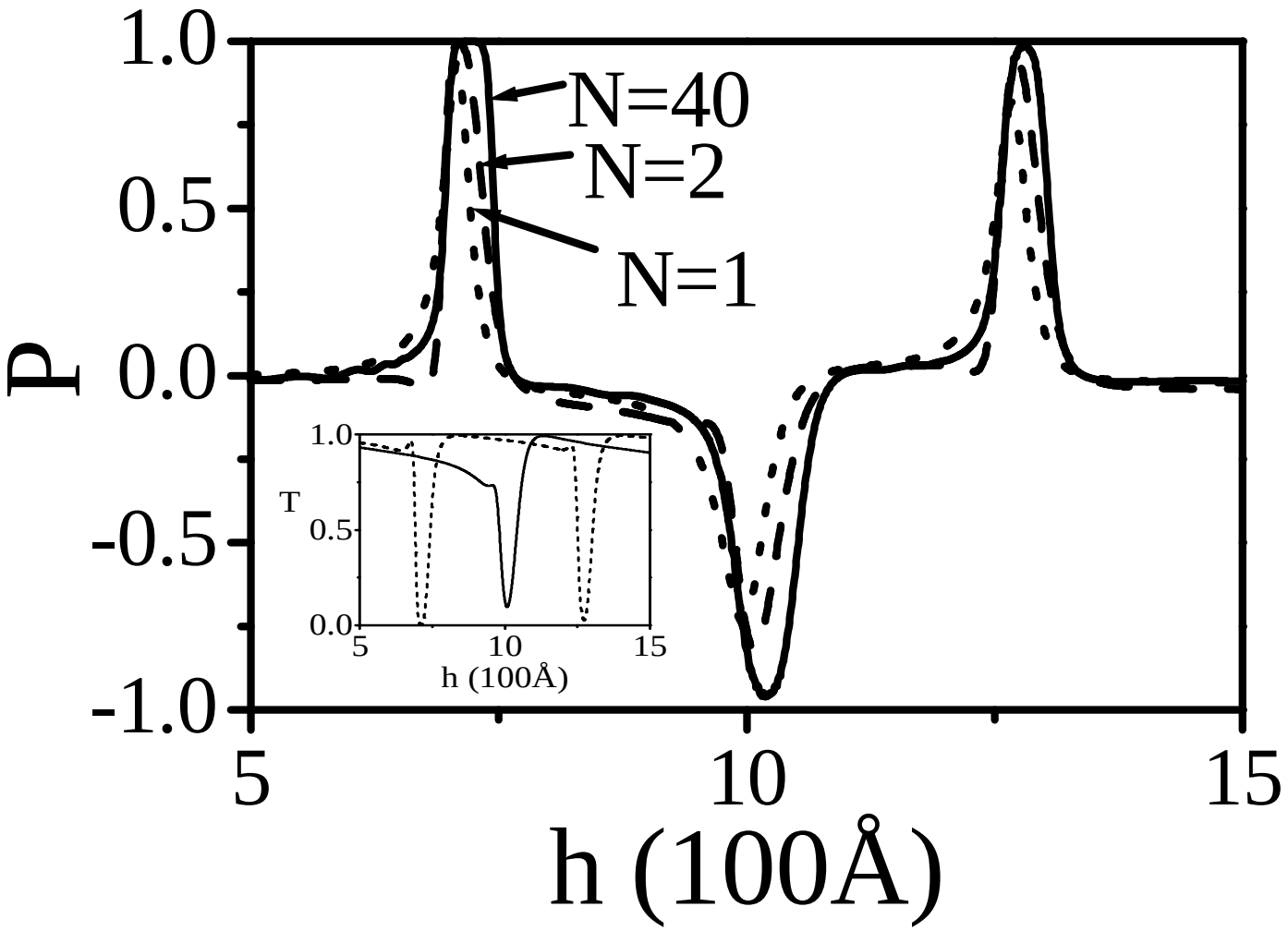

Fig.4, Wang and Vasilopoulos

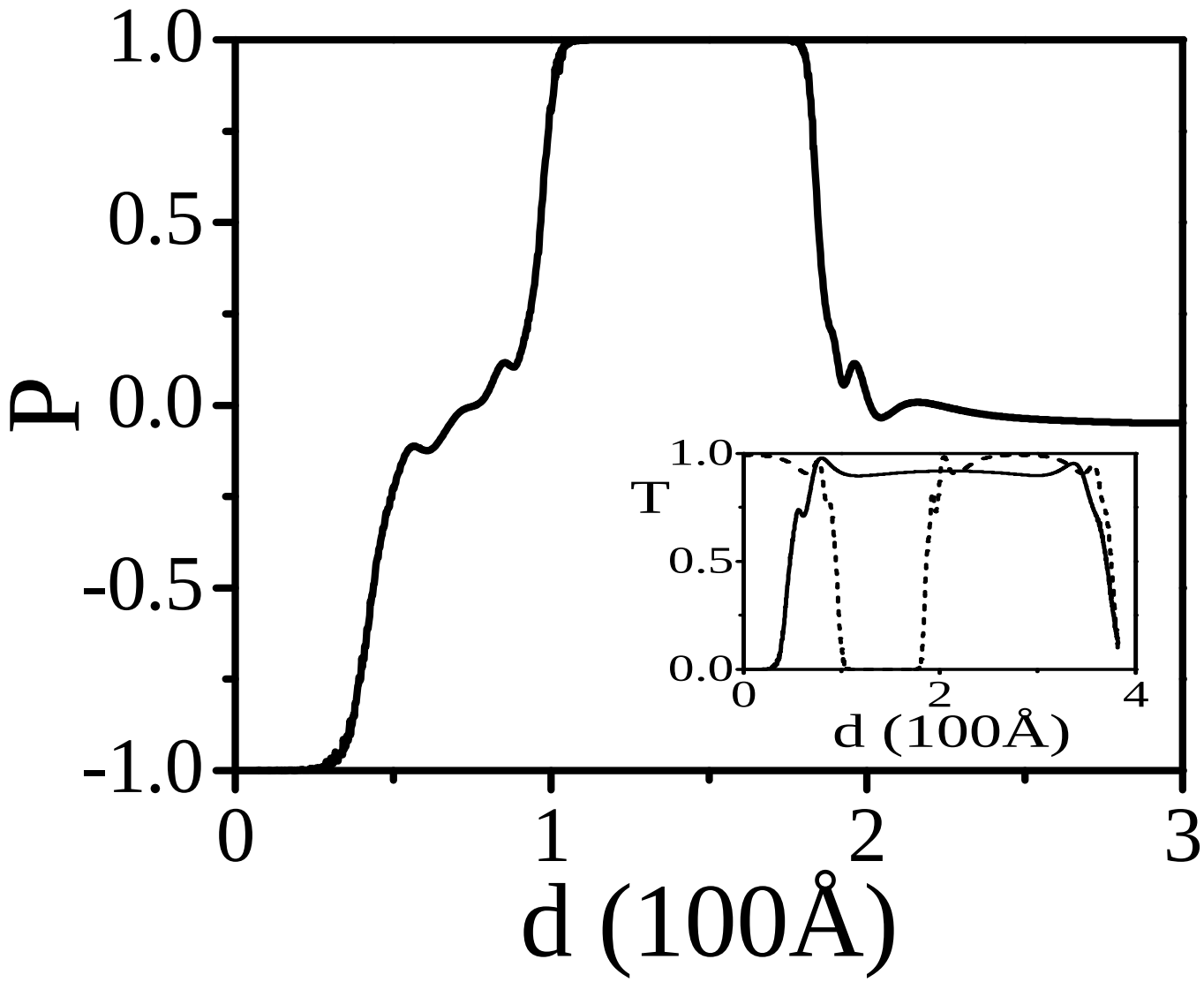

Fig.5, Wang and Vasilopoulos